

# VIBRATION ANALYSIS OF CRACK DEVELOPED ON BRIDGES USING ANSYS

Meghdivya Tandon <sup>1\*</sup>, Dr. Umank Mishra <sup>2</sup>

<sup>1</sup>M. Tech. Student, Department of Civil Engineering, Shri Shankaracharya Technical Campus, Bhilai (C.G.), India.

<sup>2</sup>Assistant Professor, Department of Civil Engineering, Shri Shankaracharya Technical Campus, Bhilai (C.G.), India.

## Abstract

The cracks induced in bridge may result in change of natural frequency. This change in natural frequency may cause damage in case of resonance which causes amplitude build up. It is therefore necessary to determine the effect of crack on natural frequency of straight bridge. The objective of current research is to investigate the effect of crack design parameters on vibrational characteristics of bridge. CAD modeling of straight bridge using ANSYS design modeler. Free vibration (modal analysis) analysis on base design of curved bridge to determine natural frequencies and mode shapes. Study on effect of I shaped steel girder dimension on vibration characteristics of bridge using Taguchi response surface method. Inducing single crack on base design and reconducting modal analysis to determine mode shapes and natural frequencies Study on effect crack dimensions parameters on vibration characteristics using Taguchi response surface method

**Keywords:** Bridge, CAD, Frequency, Vibration, Crack, ANSYS.

\* Corresponding author

## 1. Introduction

We recognize that all structures are part of the infrastructure and each one works together. The bridges take a special role, due its function to connect two different points, crossing valleys, rivers, lakes and cliffs. Bridges are needed on land transportation infrastructure because they connect different points that usually can be inaccessible. If we analyze a single bridge crossing a river, it can have many views, depending on each person's perspective [3]

- a. A person who lives in the city can visualize the bridge as a simple access to schools, parks and theaters, or a simple way to visit a family member.
- b. An engineer or architect visualizes the bridge as a way to connect the road with two points of the city, such as hospitals or fire stations.
- c. From the business community, the bridge can be viewed as access to different areas for trade, distribution of goods and services.

Depending on the needs of the society to have a bridge, it would be its importance. A bridge that serves as a quick link to recreational parks with a low traffic flow will have less impact than a bridge crossing a large river and connecting two points of the city with high traffic flow [1]. Taking into account the sentence above, we can realize that bridges are not built arbitrarily; a whole planning should be performed including design, construction, operation and maintenance of the structures.

**FEM and ANSYS**

The FEM technique is a beneficial tool for calculating mathematical equations in a variety of engineering problems. The method was suggested in the aerospace industry as a tool designed for assessing anxiety in challenging jet systems. It is developed from the matrix analysis procedure, which is utilized in aircraft design. Each researcher and practitioner has made significant progress in their respective fields. The finite element methodology's main principle is to break down a body otherwise structure into smaller, finite-size components known as limited elements.' The variables associated with a limited set of connections known as nodes or nodal points are investigated in the initial frame and structure

**2. Methodology**

The first step involves material definition. The geometry analysed comprises of structural steel material and concrete material. The material properties of structural steel are shown in figure 4.1 below. The material properties of steel are taken from ANSYS library file [43].

Properties of Outline Row 5: Structural Steel				
	A	B	C	D E
1	Property	Value	Unit	
2	Material Field Variables	Table		
3	Density	7850	kg m <sup>-3</sup>	
4	Isotropic Secant Coefficient of Thermal Expansion			
5	Coefficient of Thermal Expansion	1.2E-05	C <sup>-1</sup>	
6	Isotropic Elasticity			
7	Derive from	Young'...		
8	Young's Modulus	2E+11	Pa	
9	Poisson's Ratio	0.3		
10	Bulk Modulus	1.6667E+11	Pa	
11	Shear Modulus	7.6923E+10	Pa	

Figure 1. Steel Material Properties [43]

Properties of Outline Row 4: concrete paper				
	A	B	C	D E
1	Property	Value	Unit	
2	Material Field Variables	Table		
3	Density	2448	kg m <sup>-3</sup>	
4	Isotropic Elasticity			
5	Derive from	Young'...		
6	Young's Modulus	28000	MPa	
7	Poisson's Ratio	0.2		
8	Bulk Modulus	1.5556E+10	Pa	
9	Shear Modulus	1.1667E+10	Pa	

Figure 2. Concrete Material Properties [44]

The material properties of concrete for bridge deck are shown in figure 5 below. The material properties of concrete are taken from literature [44].

The CAD model of bridge along with I shaped girder is developed in ANSYS design modeller using sketch and extrude tools. Initially bridge deck is modelled followed by I shaped girders. The dimensional variables are defined in ANSYS design modeller. These dimension variables are H1 and V2 as shown in figure 4.3 below. H1 is the width of girder and V2 is the thickness.

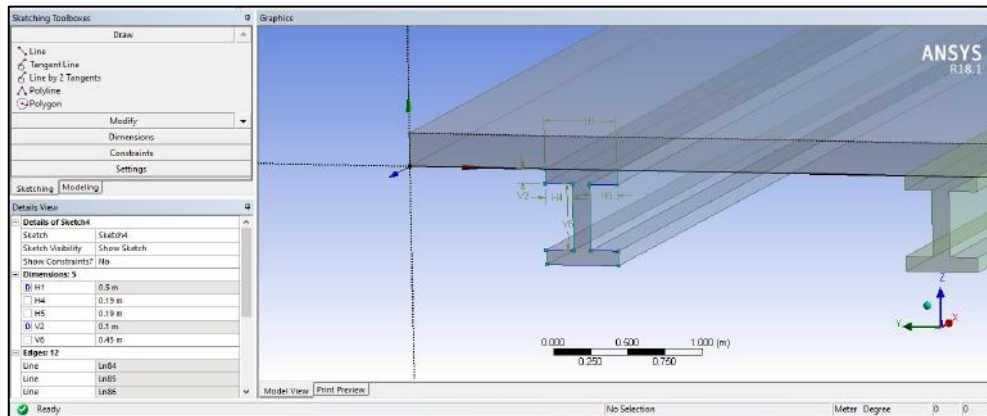


Figure 3. Selection of dimensional variables

### 2.1 Response Surface Optimization

The response surface method (RSM) is a “set of mathematical and statistical techniques that are useful for analyzing problems in which several independent variables affect a dependent variable or response” [45]. The goal is to optimize this response. “We denote the independent variables of  $X_1, X_2, X_3, X_4, \dots, X_n$  and assume that these variables are continuous and can be controlled by the experimenter with negligible error” [46]. The relationship between the dependent variable and the independent variable can be represented as

$$y = f(X_1, X_2, X_3, X_4, \dots, X_n) + \epsilon$$

where  $\epsilon$  represents the noise or error observed in the "y" response.

If we denote the expected answer with

$$E(y) = f(X_1, X_2, X_3, X_4, \dots, X_n) = \eta$$

then, the surface represented by

$$f(X_1, X_2, X_3, X_4, \dots, X_n) = \eta$$

is called the response surface [46]. The input parameters selected for optimization are shown in table 5.3 below and represented in figure below.

### 3. Result and Discussions

The vibrational analysis is conducted on bridge deck to determine natural frequencies and corresponding mode shapes. The 1st 5 natural frequencies are determined for bridge without any crack.

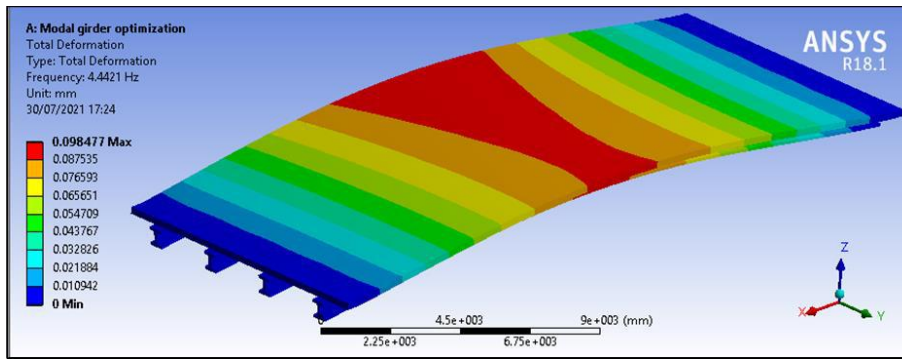


Figure 4. 1<sup>st</sup> mode shape of un-cracked geometry

The 1<sup>st</sup> natural frequency of bridge without any crack is 4.44Hz as shown in figure 5.1 above. The frequency mode shape is transverse type and maximum amplitude of deformation obtained is .0984mm.

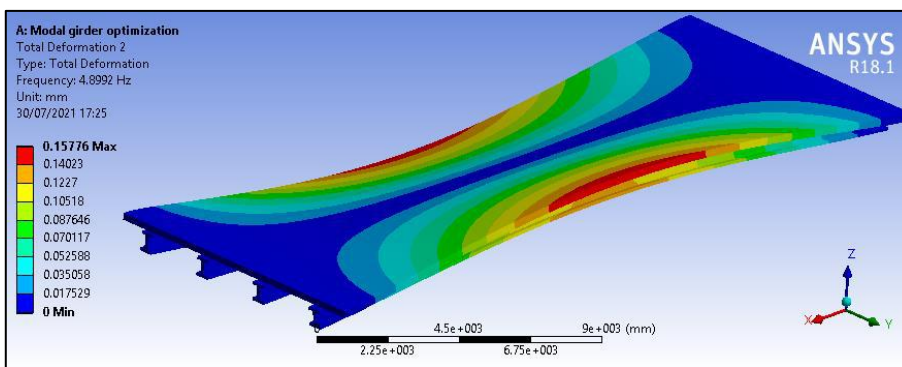


Figure 5. 2<sup>nd</sup> mode shape of un-cracked geometry

Table 1. Natural frequency comparison table

Design Type	1 <sup>st</sup> natural frequency	2 <sup>nd</sup> natural frequency	3 <sup>rd</sup> natural frequency	4 <sup>th</sup> natural frequency	5 <sup>th</sup> natural frequency
Without crack	4.4421	4.8992	9.1098	12.962	14.272
With crack	4.6439	5.0907	9.237	13.328	14.488

Table 2. Natural frequency deformation table

Design Type	1 <sup>st</sup> natural frequency	2 <sup>nd</sup> natural frequency	3 <sup>rd</sup> natural frequency	4 <sup>th</sup> natural frequency	5 <sup>th</sup> natural frequency
Without crack	.0984	.157	.183	.1018	.1609
With crack	.0991	.1586	.18394	.10233	.16061

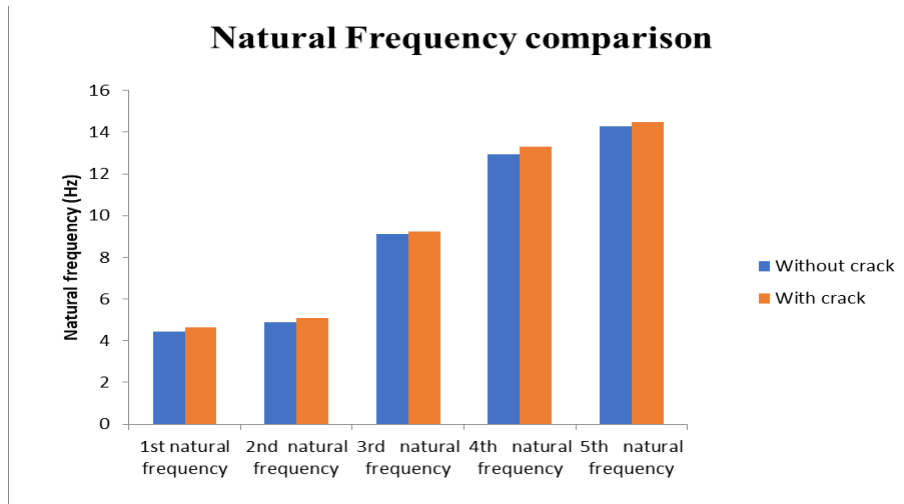


Figure 6. Natural frequency comparison

The natural frequency comparison plot is obtained from the analysis. The natural frequency of bridge without crack is observed to be higher than bridge without crack. This is observed for all the natural frequencies.

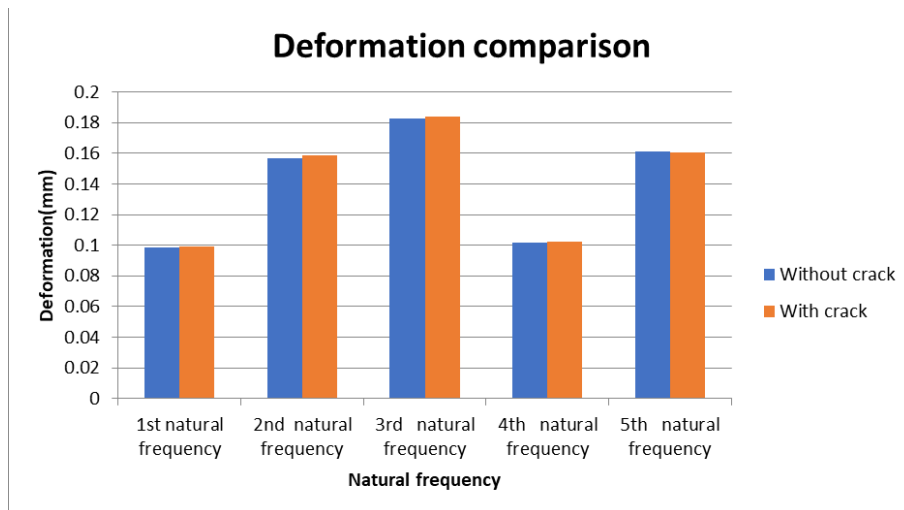


Figure 7. Natural frequency deformation comparison

The natural frequency deformation plot is obtained from the FEA analysis. For 1st 4 natural frequencies, the deformation is observed to be higher for bridge with crack and is observed to be lower for bridge without crack. For 5th natural frequency, the bridge without crack has higher deformation as compared to bridge with crack.

**3.1 Effect of girder variables on vibration characteristics (using Response Surface Optimization)**

The response surface optimization of bridge is conducted using Taguchi Design of Experiments. The design points are generated with different values of girder\_width and flange\_thickness using central composite design scheme. The design points generated are shown in chart 5.6 below. The deformation obtained for 1st, 2nd, 3rd ,4th and 5th natural frequencies are evaluated using techniques of FEA. The deformation values are shown in column D,E,F,G and H.

	A	B	C	D	E	F	G	H
1	Name	P1 - girder_width (m)	P2 - flange_thickness (m)	P3 - Total Deformation Maximum (mm)	P4 - Total Deformation 2 Maximum (mm)	P5 - Total Deformation 3 Maximum (mm)	P6 - Total Deformation 4 Maximum (mm)	P7 - Total Deformation 5 Maximum (mm)
2	1	0.5	0.1	0.098477	0.15776	0.18328	0.10186	0.16094
3	2	0.45	0.1	0.10769	0.16782	0.19328	0.11495	0.17205
4	3	0.55	0.1	0.091206	0.14947	0.1738	0.092422	0.14948
5	4	0.5	0.09	0.10022	0.16063	0.18645	0.104	0.16319
6	5	0.5	0.11	0.096983	0.15519	0.18023	0.099914	0.15889
7	6	0.45	0.09	0.10948	0.17086	0.1966	0.1175	0.17365
8	7	0.55	0.09	0.09273	0.15203	0.17685	0.094199	0.15192
9	8	0.45	0.11	0.10599	0.16493	0.19008	0.11252	0.17034
10	9	0.55	0.11	0.089722	0.14706	0.17088	0.090687	0.14727

Figure 8. DOE chart for different dimensions of girder\_width and flange\_thickness

### 3.2 Effect of crack variables on vibration characteristics (using Response Surface Optimization)

The response surface optimization of bridge with crack on I shaped girder is conducted using Taguchi Design of Experiments. The design points are generated with different values of crack\_minor and crack\_major using central composite design scheme. The design points generated are shown in chart 5.32 below. The deformation obtained for 1st, 2nd, 3rd, 4th and 5th natural frequencies are evaluated using techniques of FEA. The deformation values are shown in column D,E,F,G and H.

	A	B	C	D	E	F	G	H
1	Name	P8 - crack_minor (m)	P9 - crack_major (m)	P3 - Total Deformation Maximum (mm)	P4 - Total Deformation 2 Maximum (mm)	P5 - Total Deformation 3 Maximum (mm)	P6 - Total Deformation 4 Maximum (mm)	P7 - Total Deformation 5 Maximum (mm)
2	1 DP 0	0.018	0.09	0.099135	0.1586	0.18394	0.10233	0.16061
3	2	0.0162	0.09	0.099089	0.15859	0.18395	0.10231	0.16062
4	3	0.0198	0.09	0.098788	0.15842	0.18396	0.10212	0.16076
5	4	0.018	0.081	0.099217	0.15864	0.18392	0.10242	0.16064
6	5	0.018	0.099	0.099065	0.15856	0.18393	0.10235	0.16064
7	6	0.0162	0.081	0.098792	0.15841	0.18395	0.10219	0.16073
8	7	0.0198	0.081	0.098952	0.1585	0.18395	0.10224	0.16073
9	8	0.0162	0.099	0.099241	0.15863	0.18389	0.10243	0.16057
10	9	0.0198	0.099	0.098743	0.1584	0.18396	0.1021	0.16076

Figure 9. Design points generated for bridge with crack

## 4. Conclusion

The use of FE computer simulation is a viable tool in determining the vibrational characteristics of bridge with I shaped girders. From the modal analysis conducted on straight bridge, the type and nature of bridge deformation is determined which provided significant information on critical regions and natural frequencies. The 1st response surface optimization technique is used to determine the effect of I shaped girder design variables on vibrational characteristics. Similarly, 2nd response surface optimization technique is used to determine the effect of crack dimensions on vibrational characteristics of bridge.

The detailed findings are: -

1. From the response surface optimization on girder dimensions, it was observed that the 5<sup>th</sup> frequency maximum deformation is obtained for flange\_thickness ranging from .091mm to .109mm and girder\_width ranging from .45mm to .48mm.

2. From the response surface optimization on crack dimensions, it was observed that the maximum 5<sup>th</sup> frequency deformation is observed for crack\_major dimensions ranging from .082m to .098m and crack\_minor dimensions ranging from .019m to .0195m. The deformation is minimum for regions shown by dark blue colored region.
3. For 1<sup>st</sup> frequency deformation, crack\_minor dimension has higher sensitivity percentage (69.5%) as compared to crack\_major (23.61%) dimension which signifies that crack\_minor has higher effect on 1<sup>st</sup> frequency deformation and crack\_major has lower effect on 1<sup>st</sup> frequency deformation.
4. For 2<sup>nd</sup> frequency deformation, crack\_minor dimension has higher sensitivity percentage (70.1%) as compared to crack\_major dimension (29.9%) which signifies that crack\_minor has higher effect on 2<sup>nd</sup> frequency deformation and crack\_major has lower effect on 2<sup>nd</sup> frequency deformation.
5. For 3<sup>rd</sup> frequency deformation, crack\_minor dimension has higher sensitivity percentage (33.23%) as compared to crack\_major dimension (22.92%) which signifies that crack\_minor has higher effect on 3<sup>rd</sup> frequency deformation and crack\_major has lower effect on 3<sup>rd</sup> frequency deformation.
6. For 4<sup>th</sup> frequency deformation, crack\_minor dimension has higher sensitivity percentage (76.86%) as compared to crack\_major dimension (20.44%) which signifies that crack\_minor has higher effect on 4<sup>th</sup> frequency deformation and crack\_major has lower effect on 4<sup>th</sup> frequency deformation.
7. For 5<sup>th</sup> frequency deformation, crack\_minor dimension has higher sensitivity percentage (86.6%) as compared to crack\_major dimension (13.54%) which signifies that crack\_minor has higher effect on 5<sup>th</sup> frequency deformation and crack\_major has lower effect on 5<sup>th</sup> frequency deformation.
8. For 1<sup>st</sup> frequency deformation, the girder\_width has higher sensitivity percentage of 83.45 whereas flange\_thickness has lower sensitivity percentage of 16.39 which shows girder\_width has higher effect on 1<sup>st</sup> frequency deformation and flange\_thickness has lower effect on 1<sup>st</sup> frequency deformation.
9. For 2<sup>nd</sup> frequency deformation, the girder\_width has higher sensitivity percentage of 77.06 whereas flange\_thickness has lower sensitivity percentage of 22.75 which shows girder\_width has higher effect on 1<sup>st</sup> frequency deformation and flange\_thickness has lower effect on 2<sup>nd</sup> frequency deformation.
10. For 3<sup>rd</sup> frequency deformation, the girder\_width has higher sensitivity percentage of 75.77 whereas flange\_thickness has lower sensitivity percentage of 24.15 which shows girder\_width has higher effect on 1<sup>st</sup> frequency deformation and flange\_thickness has lower effect on 3<sup>rd</sup> frequency deformation.
11. For 4<sup>th</sup> natural frequency deformation, the girder\_width has higher sensitivity percentage of 83.94 whereas flange\_thickness has lower sensitivity percentage of 15.28 which shows girder\_width has

higher effect on 1<sup>st</sup> frequency deformation and flange\_thickness has lower effect on 4<sup>th</sup> frequency deformation.

12. For 5<sup>th</sup> natural frequency deformation, the girder\_width has higher sensitivity percentage of 85.51 whereas flange\_thickness has lower sensitivity percentage of 16.28 which shows girder\_width has higher effect on 1<sup>st</sup> frequency deformation and flange\_thickness has lower effect on 4<sup>th</sup> frequency deformation.

## References

- [1] American Society of Civil Engineers (A.S.C.E.). Infrastructure Report Card; 2017
- [2] Picture of Vidalta Cable Stayed Bridge, Mexico City. Available from: <https://www.plataformaarquitectura.cl/cl/02-304269/puente-vidalta-mexpresa>
- [3] Barker RM, Puckett JA. Design of Highway Bridges. 3rd ed. Wiley; 2013
- [4] Picture of Mexico City Road System. Available from: <https://periodicocorreo.com.mx/abren-manana-el-distribuidor-vial-en-la-glorieta-santa-fe/> [5] Picture of Forth Bridge, located on Edinburgh, Scotland. Available from: <https://www.railway-technology.com/projects/forth-rail-bridge-firthscotland/>
- [6] Picture of Golden Gate Bridge, San Francisco. Available from: <https://www.diariodelviajero.com/america/Puente-golden-gate-datos-y-curiosidades>
- [7] Picture of El Zacatal Bridge, Mexico. Available from: <http://www.sintemar.com/es/rehabilitacion-de-pilotes-enpuente-el-zacatal>
- [8] Picture of concrete piers with reinforced steel corrosion problems. Available from: [https://www.researchgate.net/figure/Concrete-structure-deteriorated-by-the-corrosion-of-steel-reinforcement\\_fig1\\_265553963](https://www.researchgate.net/figure/Concrete-structure-deteriorated-by-the-corrosion-of-steel-reinforcement_fig1_265553963)
- [9] Picture of a bridge of structural steel with corrosion problems. Available from: [https://www.researchgate.net/figure/Corrosion-of-steel-a-Extremecorrosion-in-a-bridge-b-Railway-rolling-stock-being\\_fig6\\_323826793](https://www.researchgate.net/figure/Corrosion-of-steel-a-Extremecorrosion-in-a-bridge-b-Railway-rolling-stock-being_fig6_323826793)
- [10] Picture of a bridge concrete construction joint damage. Available from: [https://www.researchgate.net/figure/Damage-at-a-joint-on-the-bridge-deck\\_fig3\\_281864780](https://www.researchgate.net/figure/Damage-at-a-joint-on-the-bridge-deck_fig3_281864780)
- [11] Picture of a girder with fatigue fracture. Available from: [https://www.researchgate.net/figure/Fatigue-fracture-failure-of-composite-beam2-images-by-S-S-Badie-and-M-KTadros\\_fig1\\_262973062](https://www.researchgate.net/figure/Fatigue-fracture-failure-of-composite-beam2-images-by-S-S-Badie-and-M-KTadros_fig1_262973062)
- [12] Zhang H, Wei X, Ding Y, Jiang Z, Ren J (2019e) A low noise capacitive MEMS accelerometer with anti-spring structure. *Sensors Actuators A: Phys* 296:79–86 Elsevier Science SA, Lausanne
- [13] Carreras L, Renart J, Turon A, Costa J, Bak BL, Lindgaard E, Martin de la Escalera F, Essa Y (2019) A benchmark test for validating 3D simulation methods for delamination growth under quasi-static and fatigue loading. *Compos Struct* 210: 932–941 Elsevier Sci Ltd, Oxford
- [14] Sun J, Zhen Z (2019) Application of infrared thermal imaging technology to steel structure coating inspection for bridges. *World Bridge* 47(05):69–73

- [15] Su S, Ge J, Wang W, Guo H, Li C, Hu J (2019b) Experimental research on the corresponding relationship between stress concentration and magnetic memory effect of steel I-column of gabled framed. *J Xian Univ Architect Technol Nat Sci Ed* 51(06):771–774+796
- [16] Ghassemi P, Toufigh V (2020) Durability of epoxy polymer and ordinary cement concrete in aggressive environments. *Constr Build Mater* 234:UNSP 117887 Elsevier Sci Ltd, Oxford
- [17] Zhou J, Zhao Y, He Q, Zhang P, Zhang H (2019b) Corrosion test of galvanized steel strand based on magnetic memory. *J Chang'an Univ Nat Sci Ed* 39(01):81–89
- [18] Macho M, Ryjacek P, Matos J (2019) Fatigue life analysis of steel riveted rail bridges affected by corrosion. *Struct Eng Int* 29(4): 551–562 Taylor & Francis Ltd, Abingdon
- [19] Gao Z, Ruan H, Qin S, Ma R, Mei D (2019) Technical status, challenges, and solutions of marine bridge engineering. *Eng Sci* 21(3):1–4 (In Chinese)
- [20] Cui C, Zhang Q, Bao Y, Bu Y, Luo Y (2019a) Fatigue life evaluation of welded joints in steel bridge considering residual stress. *J Constr Steel Res* 153:509–518 Elsevier Sci Ltd, Oxford
- [21] Y.C. Yang, S. Nagarajaiah, Blind identification of damage in time-varying systems using independent component analysis with wavelet transform, *Mech. Syst. Signal Process.* 47 (1) (2014) 3–20.
- [22] N.E. Huang, *The Hilbert-Huang Transform in Engineering*, New York, NY, USA: Taylor and Francis Group, 2005.
- [23] Y.F. Dong, Y.M. Li, L. Ming, Structural damage detection using empirical-mode decomposition and vector autoregressive moving average model, *Soil Dyn. Earthq. Eng.* 30 (3) (2010) 133–145.
- [24] C.X. Bao, H. Hao, Z.X. Li, Multi-stage identification scheme for detecting damage in structures under ambient excitations, *Smart Mater. Struct.* 22 (4) (2013) 045006.
- [25] J.P. Han, P.J. Zheng, H.T. Wang, Structural modal parameter identification and damage diagnosis based on Hilbert-Huang transform, *Earthq. Eng. Eng. Vib.* 13 (2013) 101–111.
- [26] H. Aied, A. González, D. Cantero, Identification of sudden stiffness changes in the acceleration response of a bridge to moving loads using ensemble empirical mode decomposition, *Mech. Syst. Signal Process.* 66 (2016) 314–338.
- [27] H. Li, D.W. Tao, Y. Huang, Y. Huang, A data-driven approach for seismic damage detection of shear-type building structures using the fractal dimension of time–frequency features, *Struct. Control Health Monit.* 20 (9) (2013) 1191–1210.
- [28] D. Hester, A. González, A wavelet-based damage detection algorithm based on bridge acceleration response to a vehicle, *Mech. Syst. Signal Process.* 28 (2012) 145–166.
- [29] N. Roveri, A. Carcaterra, Damage detection in structures under traveling loads by Hilbert–Huang transform, *Mech. Syst. Signal Process.* 28 (2012) 128–144.
- [30] A. Kunwar, R. Jha, M. Whelan, K. Janoyan, Damage detection in an experimental bridge model using Hilbert–Huang transform of transient vibrations, *Struct. Control Health Monit.* 20 (1) (2013) 1–15.
- [31] S.J.S. Hakim, H.A. Razak, Structural damage detection of steel bridge girder using artificial neural networks and finite element models, *Steel Compos. Struct.* 14 (4) (2013a) 367–377

- [32] A.C. Neves, I. González, J. Leander, R. Karoumi, Structural health monitoring of bridges: a model-free ANN-based approach to damage detection, *J. Civil Struct. Health Monit.* 7 (2017) 689–702.
- [33] Kim C. Y., Jung D. S., Kim N. S., Kwon S. D., Feng M. Q. Effect of vehicle weight on natural frequencies of bridges measured from traffic-induced vibration. *Earthquake Engineering and Engineering Vibration*, Vol. 2, Issue 1, 2003, p. 109-115.
- [34] Fu C. Dynamic behavior of a simply supported bridge with a switching crack subjected to seismic excitations and moving trains. *Engineering Structures*, Vol. 110, 2016, p. 59-69.
- [35] Dimarogonas A. D. Vibration of cracked structures: a state of the art review. *Engineering Fracture Mechanics*, Vol. 55, 1996, p. 831-57.
- [36] [4] Haisty B. S., Springer W. T. A general beam element for use in damage assessment of complex structures. *Journal of Vibration and Acoustics*, Vol. 110, Issue 3, 1988, p. 389-394.
- [37] Narkis Y. Identification of crack location in vibrating simply supported beams. *Journal of Sound and Vibration*, Vol. 172, Issue 4, 1994, p. 549-558.
- [38] Christides S., Barr A. D. S. One dimensional theory of cracked Bernoulli-Euler beams. *International Journal of Mechanical Sciences*, Vol. 26, Issues 11-12, 1984, p. 639-648.
- [39] Chondros T. G., Dimarogonas A. D., Yao J. A continuous cracked beam vibration theory. *Journal of Sound and Vibration*, Vol. 215, Issue 1, 1998, p. 17-34.
- [40] Yang F., Swamidass A. S. J., Seshadri R. Crack identification in vibrating beams using the energy method. *Journal of Sound and Vibration*, Vol. 244, Issue 2, 2001, p. 339-357.
- [41] Saavedra P. N., Cuitino L. A. Crack detection and vibration behavior of cracked beams. *Computers and Structures*, Vol. 79, Issue 16, 2001, p. 1451-1459.
- [42] Lin H. P., Chang S. C., Wu J. D. Beam vibrations with an arbitrary number of cracks. *Journal of Sound and Vibration*, Vol. 258, Issue 5, 2002, p. 987-999.
- [43] ANSYS Workbench Library
- [44] Radek Wodzinowski, “Free vibration analysis of horizontally curved composite concrete-steel I girder bridges” *Journal of Constructional Steel Research* 140 (2018) 47–61
- [45] M. Avalor, G. Chiandussi, and G. Belingardi, “Design optimization by response surface methodology: application to crashworthiness design of vehicle structures,” *Struct. Multidiscip. Optim.*, vol. 24, no. 4, pp. 325–332, 2002, doi: 10.1007/s00158-002-0243-x.
- [46] A. Y. A. E.-V. Silva, “Utilization of Response Surface Methodology in Optimization of Extraction of Plant Materials,” Rijeka: IntechOpen, 2018, p. Ch. 10.